

CIC-14 REPORT COLLECTION
**REPRODUCTION
COPY**

LAMS-2713

C.B

**LOS ALAMOS SCIENTIFIC LABORATORY
OF THE UNIVERSITY OF CALIFORNIA ○ LOS ALAMOS NEW MEXICO**

A DESCRIPTION OF A TIME DEPENDENT
RADIATION HYDRODYNAMICS TRANSPORT CODE
AND SOME NUMERICAL RESULTS

LOS ALAMOS NATL LAB LIBS
3 9338 00371 1313

LEGAL NOTICE

This report was prepared as an account of Government sponsored work. Neither the United States, nor the Commission, nor any person acting on behalf of the Commission:

A. Makes any warranty or representation, expressed or implied, with respect to the accuracy, completeness, or usefulness of the information contained in this report, or that the use of any information, apparatus, method, or process disclosed in this report may not infringe privately owned rights; or

B. Assumes any liabilities with respect to the use of, or for damages resulting from the use of any information, apparatus, method, or process disclosed in this report.

As used in the above, "person acting on behalf of the Commission" includes any employee or contractor of the Commission, or employee of such contractor, to the extent that such employee or contractor of the Commission, or employee of such contractor prepares, disseminates, or provides access to, any information pursuant to his employment or contract with the Commission, or his employment with such contractor.

Printed in USA. Price \$ 1.00. Available from the
Office of Technical Services
U. S. Department of Commerce
Washington 25, D. C.

LAMS-2713
PHYSICS
TID-4500 (18th Ed.)

LOS ALAMOS SCIENTIFIC LABORATORY
OF THE UNIVERSITY OF CALIFORNIA LOS ALAMOS NEW MEXICO

REPORT WRITTEN: August 1962

REPORT DISTRIBUTED: October 16, 1962

A DESCRIPTION OF A TIME DEPENDENT
RADIATION HYDRODYNAMICS TRANSPORT CODE
AND SOME NUMERICAL RESULTS

Work done by:

W. J. Byatt
R. E. Martin
T. L. Swihart

Report written by:

W. J. Byatt

Contract W-7405-ENG. 36 with the U. S. Atomic Energy Commission

All LAMS reports are informal documents, usually prepared for a special purpose and primarily prepared for use within the Laboratory rather than for general distribution. This report has not been edited, reviewed, or verified for accuracy. All LAMS reports express the views of the authors as of the time they were written and do not necessarily reflect the opinions of the Los Alamos Scientific Laboratory or the final opinion of the authors on the subject.

LOS ALAMOS NATIONAL LABORATORY



3 9338 00371 1313



ABSTRACT

A description of a time-dependent radiation transport code is given. The transport equation is written in a form such that the flow of radiation is along the characteristics in space-time. Energy conservation, the equation of state, and the hydrodynamic equations are written in a finite difference form.

Numerical results to several problems of varying degrees of complexity are given.

ACKNOWLEDGEMENTS

We should like to thank Burton Wendroff, Walter D. Barfield, and Arthur Cox for their considerable help at various stages of the work.

1. INTRODUCTION

There will be described in this report a time-dependent radiation transport code which has been written for the IBM 7030 (Stretch) computer. Numerical results for several representative problems are presented.

It is known that radiation transport phenomena in the presence of black body sources (and hydrodynamic motions) are described by a system of coupled non-linear equations. The monochromatic intensity of radiation at a space-time point travelling in a specified direction is the sum of three terms in the general case. The first is the unabsorbed and unscattered radiation reaching that point while the remaining two contributions arise from radiation scattered into the beam and emitted from the matter into the beam. The contribution to the intensity from the matter depends non-linearly on the local temperature, while the temperature itself depends on various angular moments of the intensity.

An additional peculiarity of the description of radiation transport arises in the present work due to the fact that we write the transport equation in an Eulerian frame while writing the equations of hydrodynamics in a Lagrangian coordinate system fixed in the matter. To be consistent, it is preferable (and, indeed, necessary) to transform the description of phenomena to a single frame. If one refers the radiation to the Lagrangian frame associated with the matter, the result is to introduce terms of order v/c raised to various powers. A cursory discussion of this point is given below together with references to more complete expositions.

When discussing the coding of the various equations of transport, the question of notation arises. We have not used any particular notation consistently in the report, preferring to write equations in a form which, hopefully, brings out most clearly the physical significance.

In Section 2, the equations of radiation transport are written down and put into a form suitable for transition to mesh equations. The latter are discussed in Section 3, and simplified flow diagrams are included. The presentation and discussion of numerical results is the content of Section 4.

2. THE EQUATIONS OF TRANSPORT

As radiation passes through matter, some of it is absorbed and some is scattered. That which is absorbed gives rise to a temperature distribution in the matter; emission at the local temperature then takes place. The pressure within the matter changes according to an equation of state relating the pressure and temperature. As the pressure builds up, hydrodynamic motions ensue. Energy in the system of matter plus radiation is conserved, the governing equation being the first law of thermodynamics. Thus, when speaking of radiation transport, a system of equations is needed.

Under the assumption of azimuthal symmetry, the space-time behavior of the intensity of radiation is governed by an equation of the form

$$\frac{1}{c} \frac{\partial I^\nu}{\partial t} + (\vec{I} \cdot \nabla + \sigma) I^\nu = \sigma_a^\nu B^\nu + \sigma_s \int_{-1}^1 k(\mu, \mu') I^\nu d\mu'. \quad (2.1)$$

In equation (2.1), $I^\nu = I^\nu(x, \mu, t)$ is the monochromatic intensity of radiation of frequency in the interval $d\nu$ about ν which is at a point x at time t , travelling in direction $\mu = \cos \theta$; c is the velocity of light; $\sigma = \sigma_a^\nu + \sigma_s$, where σ_a^ν is the absorption cross section of the matter for radiation of frequency ν corrected for stimulated emission, and σ_s is the scattering cross section. The quantity B^ν is taken to be a black body source at a temperature T ;

$$B^\nu = \frac{2h\nu^3}{c^2} \frac{1}{e^{h\nu/kT} - 1}. \quad (2.2)$$

The quantity $k(\mu, \mu')$ is the single scattering law. If this be assumed isotropic, then the integral on the right hand side of (2.1) reduces to

$$\frac{1}{2} \int_{-1}^1 I^\nu d\mu'; \quad (2.1a)$$

while if the Rayleigh (Thomson) law is assumed to hold, one has

$$\int_{-1}^1 k I^\nu d\mu' = \frac{3}{16} \left((3-\mu^2) \int_{-1}^1 I^\nu d\mu' + (3\mu^2-1) \int_{-1}^1 \mu'^2 I^\nu d\mu' \right). \quad (2.1b)$$

We have considered only these two scattering laws. Finally, the operator $\vec{l} \cdot \nabla$ appearing in (2.1) is geometry dependent. For plane geometry, one has

$$\vec{l} \cdot \nabla = \mu \frac{\partial}{\partial x}; \quad (2.3a)$$

while for spherical geometry, the form is

$$\vec{l} \cdot \nabla = \mu \frac{\partial}{\partial x} + \frac{(1-\mu^2)}{x} \frac{\partial}{\partial \mu}. \quad (2.3b)$$

(In this last relation, x is a spherical position coordinate.)

There are certain quantities which are of importance in a discussion of radiation transport, and which will now be defined.

The radiation energy density is defined as

$$E_r(x, t) = \frac{2\pi}{c} \int_0^{\infty} d\nu \int_{-1}^1 I^{\nu} d\mu. \quad (2.4)$$

The flux of radiation is defined as

$$F(x, t) = 2\pi \int_0^{\infty} d\nu \int_{-1}^1 \mu I^{\nu} d\mu. \quad (2.5)$$

The mean intensity of radiation is defined as

$$J(x, t) = \int_0^{\infty} d\nu \int_{-1}^1 \bar{I} d\mu. \quad (2.6)$$

Finally, the radiation pressure is given by the relation

$$p_r = \frac{2\pi}{c} \int_0^{\infty} d\nu \int_{-1}^1 \mu^2 I^{\nu} d\mu. \quad (2.7)$$

The pressure is connected with the temperature and density within the matter by an equation of state; i.e.,

$$p_m = f(\rho, T). \quad (2.8)$$

For the cases which we have considered thus far, we have used a perfect gas law such that

$$p_m = b \rho T, \quad (2.8a)$$

with b defined as the gas constant in units of energy per unit mass per degree.

There is one additional matter which deserves mention. When one considers multi-group problems, it is necessary to define

some sort of average of the absorption coefficient over finite frequency groups. Suppose that we integrate equation (2.1) over a range of frequencies from ν_1 to ν_2 . Calling

$$\int_{\nu_1}^{\nu_2} I^\nu d\nu = I^g(x, \mu, t),$$

equation (2.1) is

$$\frac{1}{c} \frac{\partial I^g}{\partial t} + (\vec{l} \cdot \nabla) I^g + \sigma_s I^g = \int_{\nu_1}^{\nu_2} \sigma_a^\nu (B^\nu - I^\nu) d\nu + \sigma_s \int_{-1}^1 k I^g d\mu',$$

If it were possible to compute a mean-absorption coefficient defined by

$$\bar{\sigma}_a^g (B^g - I^g) = \int_{\nu_1}^{\nu_2} \sigma_a^\nu (B^\nu - I^\nu) d\nu, \quad (2.9)$$

then the transport equation, integrated between two frequencies, would take the form

$$\frac{1}{c} \frac{\partial I^g}{\partial t} + (\vec{l} \cdot \nabla) I^g + (\bar{\sigma}_a^g + \sigma_s) I^g = \bar{\sigma}_a^g B^g + \sigma_s \int_{-1}^1 k I^g d\mu'. \quad (2.10)$$

Mean absorption coefficients other than (2.9) have some validity.

Chief among these are the well known Rosseland mean, valid when the approximations of diffusion theory hold, and the so-called Planck mean given by

$$\bar{\sigma}_a^g B^g = \int_{\nu_1}^{\nu_2} \sigma_a^\nu B^\nu d\nu. \quad (2.11)$$

It is the mean defined by equation (2.11), valid when mean free paths are long, which we have used for the most part. The question of how best to define a mean which will be valid in both the short and long mean free path limit is being considered by both B. Wendroff and W. D. Barfield of LASL.

Since the frame to which the matter is attached (by means of a Lagrangian coordinate description) will be moving with some velocity \vec{v} , it is necessary to look into the question of the effects which such motion will have on the transport equation when it is referred to the matter frame.

This problem was discussed by L. H. Thomas (1), and more recently by A. N. Fraser (2). In addition, Ledoux and Walraven (3) have material bearing on such transformations in their Handbuch article.

The use of the two scattering laws which have been assumed valid in this report introduces an important simplification when discussing energy conservation; namely, the scattering cancels out exactly. (For temperatures high enough so that the Klein-Nishina formula is the only valid one, this is not so.) We can, therefore, discuss energy conservation starting with a transport equation in the form

$$\frac{1}{c} \frac{\partial I^\nu}{\partial t} + \vec{l} \cdot \nabla I^\nu = \sigma_a^\nu (B^\nu - I^\nu). \quad (2.12)$$

Recalling the definitions (2.4) and (2.5), it will be seen that the result of multiplying (2.12) by 2π and then integrating over all μ and ν is to form

$$\frac{\partial E_r}{\partial t} + \nabla \cdot F = \int_0^\infty \sigma_a^\nu d\nu (4\pi B^\nu - cE_r^\nu). \quad (2.13)$$

The right-hand-side of (2.13) is a measure of the heat added to the material per unit volume per unit time. A difficulty arises. Equation (2.12) is written in Eulerian form. We shall follow the material via the Lagrangian prescription. The material will, in general, be flowing with some velocity v relative to the fixed Eulerian frame. The radiation flows with the speed of light. Intuitively, one feels that corrections of the order of v/c will appear if (2.13) is now transformed to a frame fixed in the matter. This is, in fact, the case. However, the ratio of v/c will be no greater than $1/300$, and will be, in general, much less. Thus, we shall ignore the correction terms. Then (2.13) can be written in the form

$$\frac{\partial E_r}{\partial t} + \nabla \cdot F = - \frac{dQ}{dt},$$

which, by the first law of thermodynamics becomes

$$\frac{\partial E_r}{\partial t} + \nabla \cdot F = - \left\{ \rho \frac{d}{dt} \left(\frac{E_m}{\rho} \right) + \rho p \frac{d}{dt} \left(\frac{1}{\rho} \right) \right\}.$$

Using the continuity equation, and the equation of motion, one can write this last in the form

$$\frac{d}{dt} \left(\frac{E_m + E_r + \frac{1}{2} \rho v^2}{\rho} \right) = -\frac{1}{\rho} \nabla \cdot (F + p_T V), \quad (2.13a)$$

where $E_m = \rho c_v T$ for a perfect gas and $\frac{1}{2} \rho v^2$ is the specific kinetic energy of the material. The quantity p_T is the total pressure, given by

$$p_T = p_m + p_r + p_{visc.}$$

Concerning the viscous pressure, more will be said later.

Using a Lagrangian coordinate system, the mass per zone is a constant. Knowing the pressure from the equation of state, forces on a unit area of a zone interface can be computed. Knowing the (constant) mass, we can then find the acceleration of the material. By integrating, the velocity and position of interfaces at some later time can then be found. Knowing these last, we can then compute new densities and temperatures through the system and once again find new pressures from the equation of state. The finite-difference equations for hydrodynamics will be discussed in Section 3.

It is the intent of this section as mentioned earlier to put the system of equations into a form suitable for numerical manipulation. We have used equation (2.13a), together with the hydrodynamic equations in finite-difference form. The equation of radiation transport, (2.1), will now be discussed further. Whether the operator $\vec{l} \cdot \nabla$ has the form (2.3a) or (2.3b), we make the substitution

$$\frac{1}{c} \frac{\partial}{\partial t} + \vec{l} \cdot \nabla = \frac{d}{ds}. \quad (2.14)$$

This is equivalent to insisting that the independent variables x, μ, t depend on the parameter s . The expressions for $x(s), \mu(s), t(s)$ are the equations of the characteristics along which the radiation flows in space-time. In plane geometry,

$$\frac{d}{ds} = \frac{1}{c} \frac{\partial}{\partial t} + \mu \frac{\partial}{\partial x}$$

implies that

$$\left. \begin{aligned} \frac{dt}{ds} = \frac{1}{c}, \quad \frac{dx}{ds} = \mu, \end{aligned} \right\}$$

and that

$$\frac{d\mu}{ds} = 0.$$

(2.15)

The solution to the set (2.15) yields

$$\left. \begin{aligned} x(s) &= x_0 \pm \mu s, \\ t(s) &= t_0 \pm s/c \\ \mu(s) &= \mu_0. \end{aligned} \right\} \quad (2.16)$$

In spherical geometry,

$$\frac{d}{ds} = \frac{1}{c} \frac{\partial}{\partial t} + \mu \frac{\partial}{\partial x} + \frac{(1-\mu^2)}{x} \frac{\partial}{\partial \mu},$$

implying that

$$\left. \begin{aligned} \frac{dt}{ds} &= \frac{1}{c}, \quad \frac{dx}{ds} = \mu(s), \end{aligned} \right\} \quad (2.17)$$

and that

$$\frac{d\mu}{ds} = \frac{(1-\mu^2)}{x}.$$

The solution to the set (2.17) is

$$\left. \begin{aligned} x(s) &= (x_0^2 + s^2 \pm 2x_0\mu_0 s)^{1/2}, \\ t(s) &= t_0 \pm s/c, \\ \mu(s) &= (\mu_0 x_0 \pm s)/x(s). \end{aligned} \right\} \quad (2.18)$$

With the substitution (2.14), equation (2.1) can be written as

$$\frac{d\bar{I}}{ds} + \sigma \bar{I} = \sigma_a \bar{B} + \sigma_s K \bar{I}, \quad (2.19)$$

where K is a scattering operator. This can be integrated between

two points on a characteristic. One has

$$I(x(s), \mu(s), t(s)) = I(x(s_1), \mu(s_1), t(s_1)) e^{-\int_{s_1}^s \sigma ds'} + \int_{s_1}^s e^{-\int_{s_1}^{s'} \sigma ds''} \{ \sigma_a B + \sigma_s K I \} ds' \quad (2.20)$$

The radiation transport equation in the form (2.20) has been coded for use on the Stretch.

We now turn to a discussion of the mesh equations themselves.

3. THE MESH EQUATIONS AND FLOW DIAGRAMS

For the purposes of numerical computation, we label the position, angle, time and energy as x_i , μ_k , t_j , and v_g respectively, where the subscripts take on discrete values. The dependent variables are then defined as

$$\left. \begin{aligned} I^v(x, \mu, t) &= I_{ijk}^g, \\ T(x, t) &= T_{ij}, \\ p(x, t) &= p_{ij}, \end{aligned} \right\} \quad (3.1)$$

and so forth. When quantities are computed at the midpoint of zones, $i-i \pm \frac{1}{2}$, with a similar statement holding for the time.

Because of the initial and boundary value character of the problems, data along the lines $x_i = 0$, $t_j = 0$ must be given. For the sake of being definite, imagine that we are discussing a problem in plane geometry. Supposing further that no unbalanced hydrodynamic forces are present, so that the relative positions of

the x_i are time-independent, a mesh such as is shown in Fig. 1 can be constructed.

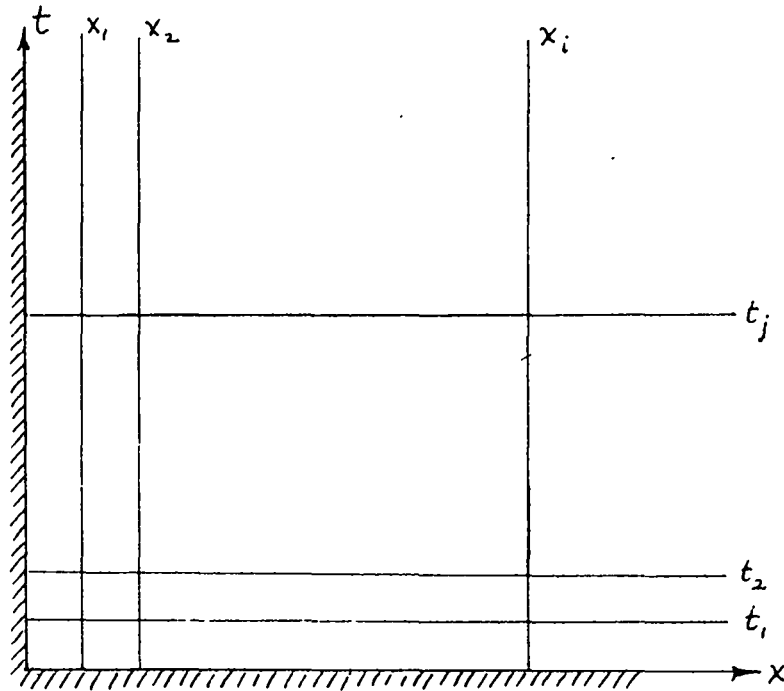


Fig. 1
Mesh in the x-t Plane

The fact that initial and boundary value data are given is indicated by the cross-hatching in Fig. 1. In Fig. 2, an enlarged section of Fig. 1, the characteristics have been drawn into the mesh, together with two angles, μ_1 , μ_2 .

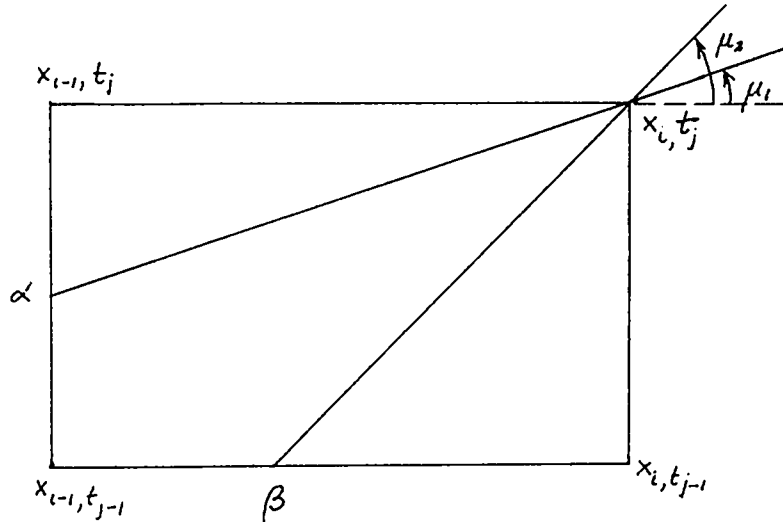


Fig. 2

An Enlarged Portion of the Mesh in the
x-t Plane

Suppose we wish to compute the intensity at the point x_i, t_j in the direction μ_1 . The characteristic, when drawn backwards, intersects the vertical line x_{i-1} at some instant of time between t_{j-1} and t_j . To compute this value of the time, observe that the distance which the photon has travelled is $(x_i - x_{i-1})/\mu_1$ so that the time associated with the point α is

$$t(\alpha) = t_j - \frac{(x_i - x_{i-1})}{\mu_1 c}. \quad (3.2)$$

Since a value of the intensity at position x_{i-1} at time $t(\alpha)$ is unknown, we use linear interpolation to obtain the approximation

$$I_\alpha = I_j + \left(\frac{t_j - t(\alpha)}{t_j - t_{j-1}} \right) (I_{j-1} - I_j). \quad (3.3)$$

On the other hand, angles such as μ_2 can exist, such that the characteristic will intersect at the point β . But

$$x(\beta) = x_i - \mu_2 c (t_j - t_{j-1}), \quad (3.4)$$

so that, analogous with (3.3), we have

$$I_\beta = I_i + \left(\frac{x_i - x(\beta)}{x_i - x_{i-1}} \right) (I_{i-1} - I_i). \quad (3.5)$$

We now want to develop the mesh equation for the intensity.

Equation (2.20) is

$$I^v(x(s), \mu(s), t(s)) = I^v(x(s_i), \mu(s_i), t(s_i)) e^{-\int_{s_i}^s \sigma^v d\xi} + \int_{s_i}^s e^{-\int_{s'}^s \sigma^v d\xi} \{ \sigma_a^v B^v + \sigma_s K I^v \} ds' \quad (2.20)$$

In the case of the characteristic intersecting at the point α , we have

$$I_{i,j,1}^g = I_\alpha^g e^{-\int_{x_{i-1}/\mu_1}^{x_i/\mu_1} \sigma^g d\xi} + \int_{x_{i-1}/\mu_1}^{x_i/\mu_1} e^{-\int_{s'}^{x_i/\mu_1} \sigma^g d\xi} \{ \sigma_a^g B^g + \sigma_s K I^g \} ds', \quad (3.6a)$$

where I_{α}^g is given by (3.3). If the point of intersection were β , one would have

$$I_{i,j,2}^g = I_{\beta}^g e^{-\int_{ct_{j-1}}^{ct_j} \sigma^g d\xi} + \int_{ct_{j-1}}^{ct_j} e^{-\int_{s'}^{ct_j} \sigma^g ds'} \{ \sigma_a^g B^g + \sigma_s K I^g \} ds'. \quad (3.6b)$$

To evaluate the term KI (which is proportional to the mean intensity) on the right hand side of (3.6a) or (3.6b), we have used the double Gaussian quadrature formula; i.e.,

$$J^g = \sum_{l=0}^n a_l I_l^g. \quad (3.7)$$

Similarly, the equations for the (monochromatic) energy, the flux, and the radiation pressure are

$$\begin{aligned} E^g &= \frac{2\pi}{c} J^g, \\ F^g &= 2\pi \sum_{l=0}^n a_l \mu_l I_l^g, \\ p_g &= \frac{2\pi}{c} \sum_{l=0}^n a_l \mu_l^2 I_l^g \end{aligned} \quad (3.8)$$

Table 1 contains the values of a_k, μ_k for various values of k .

Table 1
Table of the Zeros of the Legendre Polynomial and
the weight coefficient for Gauss integration in
the interval $0 \leq x \leq 1$

	<u>Zeros</u>		<u>Weight</u>
k=2			
x_1	.211 324 8654	a_1	.500 000 0000
x_0	.788 675 1346	a_0	.500 000 0000
k=3			
x_1	.112 701 6654	a_1	.277 777 7778
x_0	.500 000 0000	a_0	.444 444 4444
x_{-1}	.887 298 3346	a_{-1}	.277 777 7778
k=4			
x_2	.06943184420	a_2	.1739274226
x_1	.3300094782	a_1	.3260725774
x_0	.6699905218	a_0	.3260725774
x_{-1}	.9305681558	a_{-1}	.1739274226
k=5			
x_2	.04691007703	a_2	.1184634425
x_1	.2307653449	a_1	.2393143352
x_0	.500 000 0000	a_0	.2844444444
x_{-1}	.7692346550	a_{-1}	.2393143352
x_{-2}	.9530899230	a_{-2}	.1184634425

	<u>Zeros</u>		<u>Weight</u>
k=6			
x_3	.03376524290	a_3	.08566224619
x_2	.1693953068	a_2	.1803807865
x_1	.3806904070	a_1	.2339569673
x_0	.6193095930	a_0	.2339569673
x_{-1}	.8306046932	a_{-1}	.1803807865
x_{-2}	.9662347571	a_{-2}	.08566224619
k=7			
x_3	.02544604383	a_3	.06474248308
x_2	.1292344072	a_2	.1398526957
x_1	.2970774243	a_1	.1909150253
x_0	.50000 00000	a_0	.2089795918
x_{-1}	.7029225757	a_{-1}	.1909150253
x_{-2}	.8707655928	a_{-2}	.1398526957
x_{-3}	.9745539562	a_{-3}	.06474248308
k=8			
x_4	.01985507175	a_4	.05061426815
x_3	.1016667613	a_3	.1111905172
x_2	.2372337950	a_2	.1568533229
x_1	.4082826788	a_1	.1813418917
x_0	.5917173212	a_0	.1813418917

	<u>Zeros</u>		<u>Weight</u>
k=8 continued			
x ₋₁	.7627662050	a ₋₁	.1568533229
x ₋₂	.8983332387	a ₋₂	.1111905172
x ₋₃	.9801449283	a ₋₃	.05061426815
k=9			
x ₄	.01591988025	a ₄	.04063719418
x ₃	.08198444634	a ₃	.09032408035
x ₂	.1933142836	a ₂	.1303053482
x ₁	.3378732883	a ₁	.1561735385
x ₀	.50000 00000	a ₀	.1651196775
x ₋₁	.6621267117	a ₋₁	.1561735385
x ₋₂	.8066857164	a ₋₂	.1303053482
x ₋₃	.9180155537	a ₋₃	.09032408035
x ₋₄	.9840801198	a ₋₄	.04063719418
k=10			
x ₅	.01304673574	a ₅	.03333567215
x ₄	.06746831666	a ₄	.07472567458
x ₃	.1602952158	a ₃	.1095431813
x ₂	.2833023030	a ₂	.1346333597
x ₁	.4255628305	a ₁	.1477621124
x ₀	.5744371695	a ₀	.1477621124

	<u>Zeros</u>		<u>Weight</u>
k=10 continued			
x_{-1}	.7166976970	a_{-1}	.1346333597
x_{-2}	.8397047842	a_{-2}	.1095431813
x_{-3}	.9325316834	a_{-3}	.07472567458
x_{-4}	.9869532643	a_{-4}	.03333567215
k=11			
x_5	.01088567093	a_5	.02783428356
x_4	.05646870012	a_4	.06279018473
x_3	.1349239972	a_3	.09314510546
x_2	.2404519354	a_2	.1165968823
x_1	.3652284220	a_1	.1314022723
x_0	.50000 00000	a_0	.1364625434
x_{-1}	.6347715780	a_{-1}	.1314022723
x_{-2}	.7595480646	a_{-2}	.1165968823
x_{-3}	.8650760028	a_{-3}	.09314510546
x_{-4}	.9435312999	a_{-4}	.06279018473
x_{-5}	.9891143291	a_{-5}	.02783428356
k=12			
x_8	.00921968288	a_8	.02358766819
x_5	.04794137181	a_5	.0534696630
x_4	.1150486629	a_4	.08003916427
x_3	.2063410228	a_3	.1015837134

<u>Zeros</u>		<u>Weight</u>	
k=12 continued			
x_2	.3160842505	a_2	.1167462683
x_1	.4373832958	a_1	.1245735229
x_0	.5626167043	a_0	.1245735229
x_{-1}	.6839157495	a_{-1}	.1167462683
x_{-2}	.7936589772	a_{-2}	.1015837134
x_{-3}	.8849513371	a_{-3}	.08003916427
x_{-4}	.9520586282	a_{-4}	.0534696630
x_{-5}	.9907803171	a_{-5}	.02358766819

Equations (3.6a,b) can now be written in the form

$$I_{i,j,k}^g = I_{i,j,k}^g e^{-\int_0^s \sigma g d\xi} + \int_0^s e^{-\int_{s'}^s \sigma g d\xi} \{ \sigma_a g B g + \sigma_s \sum a_l I_l^g \} ds, (3.9)$$

where $s = \Delta x / \mu_k$ if $\Delta x / \mu_k \leq c \Delta t$, and $s = c \Delta t$ otherwise.

Specializing, for the sake of clarity, to the case for which $s = \Delta x / \mu_k$ and to a one energy group problem with constant σ 's (and, as stated earlier, in plane geometry), we can now write (3.9) as

$$I_{i,j,k}^g = I_{i,j,k}^g e^{-\sigma \Delta x / \mu_k} + \int_0^{\Delta x / \mu_k} e^{-\sigma x'} dx' \{ \sigma_a B + \sigma_s \sum a_l I_l \} \Big|_{x_i - \mu_k x', t_j - \frac{x'}{c}}. (3.10)$$

The integral is now evaluated by Simpson's rule. One has

$$I_{i,j,k}^q = I_{i-1,j,k} e^{-\sigma \Delta x / \mu_k} + \frac{h}{3} \left\{ \chi_{i,j,k} + 4 e^{-\sigma h} \chi(x_i - \mu_k h, t_j - \frac{h}{c}) + \dots + e^{-\sigma \Delta x / \mu_k} \chi_{i-1}(t_j - \Delta x / \mu_k c) \right\}. \quad (3.11)$$

The quantity $h = \frac{\Delta x}{n \mu_k}$, where n is some even number; the substitution $\chi = \sigma_a B + \sigma_s KI$ has been made. Now, values of χ are not known at each point between x_i and x_{i-1} . Linear interpolation of the intensity between the two values is used to obtain an approximation. Moreover, an iteration scheme must be used to obtain accurate values of the intensity since the scattering contribution is initially unknown. The iteration scheme which we have employed is as follows. When temperature dependent sources are present, we assume that $I^{(0)} = B$ as a zeroth guess. Then, from (3.11)

$$I_{i,j,k}^{(1)} = I_{i-1,j,k}^{(0)} e^{-\sigma \Delta x / \mu_k} + \frac{h}{3} \left\{ \chi_{i,j,k}^{(0)} + \dots \right\}. \quad (3.11a)$$

When an equation of the form (3.11a) is evaluated for each angle μ_k , the mean intensity $J^{(1)}$, the energy density $E^{(1)}$, and the flux $F^{(1)}$ are evaluated according to (3.8). Then, the finite difference form of the energy conservation equation is used to find a new temperature distribution. From this last, a new source is computed so that $\chi^{(1)}$ is known. From this, a new $I_{ijk}^{(2)}$ is computed and the cycle repeats until appropriate convergence criteria are

fulfilled. These are on the mean intensity where we require that

$$\frac{J^{n+1} - J^n}{\max(J^{m+1,n})} < \epsilon, \quad (3.12)$$

where n is the order of iteration, and on the temperature

$$\frac{T^{n+1} - T^n}{\max(T^{n+1,n})} < \eta. \quad (3.13)$$

Although the methods used in problems involving spherical geometry are similar, there are some peculiarities concerning the mesh.

Referring to equations (2.18), make the substitutions

$$\begin{aligned} \hat{x}(s) &= \mu(s)x(s), \\ \hat{y}(s) &= x(s)\sqrt{1-\mu^2(s)}. \end{aligned} \quad (3.14)$$

The mesh in spherical coordinates is constructed as shown in Fig. 3.

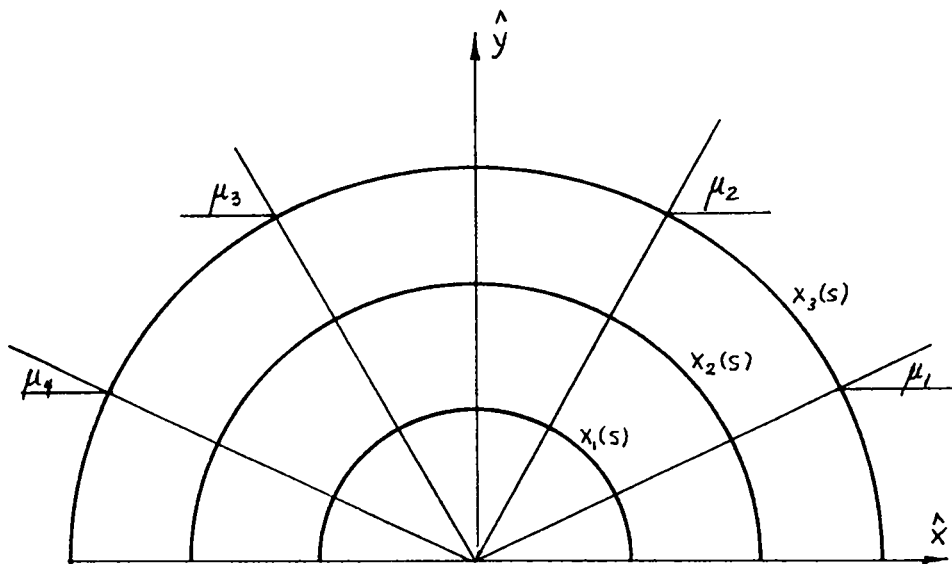


Fig. 3
Schematic Diagram of the Mesh in Spherical Coordinates

Fig. 4 is, again, an enlarged portion of the mesh, in which the quantities \hat{x} , \hat{y} , are shown, together with other details pertinent to the calculation of the intensity of radiation at the point $x_2(s)$

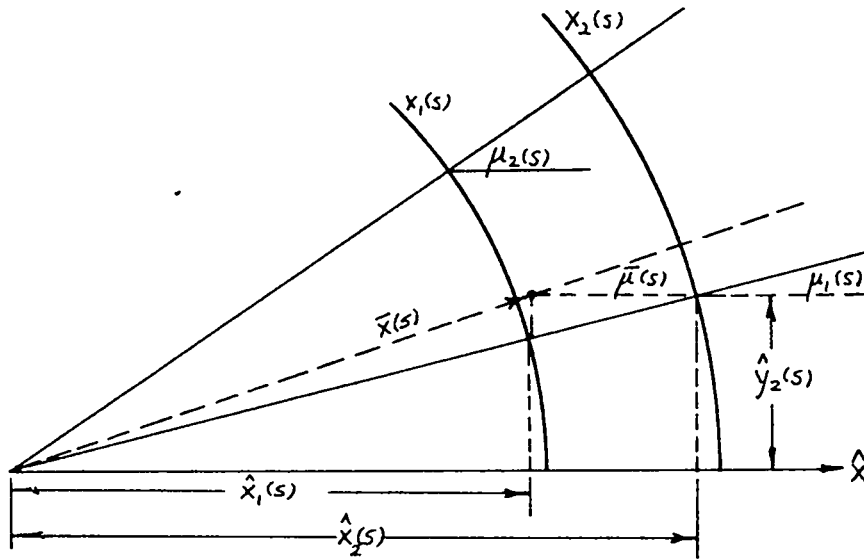


Fig. 4

Enlarged Portion of the Mesh in Spherical Coordinates

travelling in direction $\mu_1(s)$. Write the transport equation in a spherical coordinate system as

$$I^q(x_2(s), \mu_1(s), t(s)) = I^q(\bar{x}(s), \bar{\mu}(s), \bar{t}(s)) e^{-\sigma^q(\hat{x}_2 - \hat{x}_1)} + \int_{\hat{x}_1}^{\hat{x}_2} e^{-\sigma^q(\hat{x}_2 - x')} \{ \sigma_a^q B^q + \sigma_s \sum_l a_l I_l \} dx' \quad (3.15)$$

Again, a single energy group calculation with constant σ 's has been assumed.

It is a straightforward matter to find expressions for $\bar{\mu}$, \bar{x} , and \bar{t} in terms of quantities which are fixed. From Fig. 3, for example,

$$\bar{x}(s) = \sqrt{\hat{x}_1^2 + \hat{y}_2^2},$$

which, by relations (3.14) can be written as

$$\bar{x} = \sqrt{(\mu_1 x_1)^2 + x_2^2 (\sqrt{1 - \mu_2^2})^2}. \quad (3.16)$$

Further,

$$\bar{\mu}(s) = \hat{x}_1 / \bar{x} \quad (3.17)$$

can now be computed since all quantities on the right hand side of (3.16) are known. As for $\bar{t}(s)$, it is given by

$$\bar{t} = t(s) - \frac{(\hat{x}_2 - \hat{x}_1)}{c}. \quad (3.18)$$

The intensity is not known at $\bar{x}(s)$, $\bar{\mu}(s)$, $\bar{t}(s)$, but interpolation in position, angle, and time can be made to find an approximation. From this point on, the method of numerical analysis is identical with that used in the plane geometry part of the code. It is worthwhile noting, however, that our experience has indicated that the linear interpolation formulas we use make for rather slow convergence of the iterative scheme.

The mesh equations for energy balance follow directly from equation (2.13). In plane geometry, one has

$$(c_v T + E_r / \rho + v^2/2)_{i, j+1/2}^{t+\Delta t} = (c_v T + E_r / \rho + v^2/2)_{i, j+1/2}^t - \frac{\Delta t}{m_{i+1/2}} \left\{ \hat{F}_{i+1, j+1/2} - \hat{F}_{i, j+1/2} \right\}, \quad (3.19)$$

where $\hat{F} = F + vP_T$, and the perfect gas equation $E_m = \rho c_v T$ has been used. For spherical coordinates, the expression is

$$(c_v T + E_r / \rho + v^2/2)_{i, j+1/2}^{t+\Delta t} = (c_v T + E_r / \rho + v^2/2)_{i, j+1/2}^t - \frac{\Delta t}{m_{i+1/2}} \left\{ (A\hat{F})_{i+1, j+1/2} - (A\hat{F})_{i, j+1/2} \right\}, \quad (3.20)$$

where $A = 4\pi r^2$.

Hydrodynamics

The equations for hydrodynamics which we solve are, in essence, used only to compute new interface positions as a function of time. The Lagrangian coordinate system holds the mass constant in any zone and allows the density to vary. We start from Newton's second law in the form

$$\ddot{x}_i^j = 2(p_{i-1/2}^j - p_{i+1/2}^j) A_i^j / (m_{i+1/2} + m_{i-1/2}), \quad (3.21)$$

where again i denotes position and j the time; \ddot{x}_i^j is the acceleration at the point x_i at time t_j , while the p 's are pressures, A_i^j is an appropriate area, and the m 's are the preassigned, constant masses. To find the velocity of the material, we write

$$\dot{x}_i^{j+1/2} = \ddot{x}_i^j \Delta t + x_i^{j-1/2}, \quad (3.22)$$

and on integrating once more, we have the positions according to

$$x_i^{j+1} = x_i^j + \dot{x}_i^{j+1/2} \Delta t. \quad (3.23)$$

The centering of these equations minimizes truncation errors.

In plane geometry, the A_1^j are constant areas, while for spherical geometry, they are, as mentioned earlier,

$$A_1^j = 4\pi (x_i^j)^2. \quad (3.24)$$

It is necessary to exercise some care in selecting the time interval Δt ; the need arises from the fact that if Δt is too large, and if the velocities are high enough, the quantity

$$x_i^{j+1} - x_i^j$$

can become negative. Physically, of course, this is impossible, but mathematically, it is clear from examination of (3.22) and (3.23) that velocity and position are linearly dependent on Δt . We use the Courant condition to fix a maximum on Δt ; i.e.,

$$c_s \frac{\Delta t}{\Delta x} < 1. \quad (3.25)$$

Here, c_s is the sound speed in the medium.

In addition, we introduce an artificial viscosity after the fashion of von Neumann to smooth out oscillations within a zone. It is turned on when the velocities computed indicate that the material is collapsing. The form of the viscosity term

is

$$q = a \rho (\nabla \cdot v)^2 (\Delta x)^2, \quad (3.26a)$$

which is differenced as

$$q_{i+\frac{1}{2},j} = a \rho_{i+\frac{1}{2},j} (v_{i+1,j-\frac{1}{2}} - v_{i,j-\frac{1}{2}})^2 \quad (3.26b)$$

in plane coordinates and in the same manner in spherical coordinates with the proper expression for the divergence. The number a is generally taken to be two. If the shock speed becomes high, it is increased to four or more.

This completes the discussion of the mesh equations. Figs. 5 and 6 are simplified flow diagrams of parts of the code. They do not handle in any detail the subroutines by means of which quantities are computed, but simply indicate the order in which things are done.

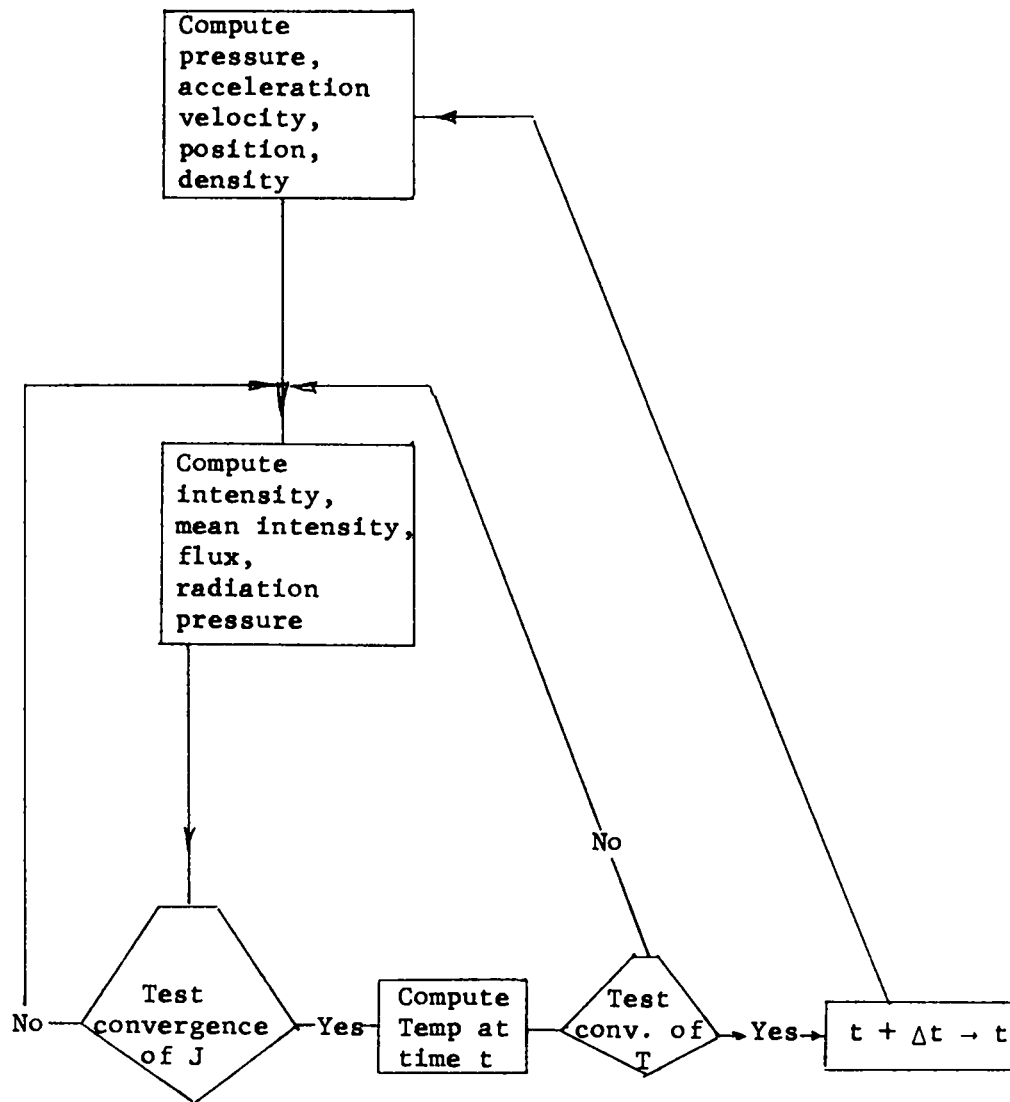


Fig. 5

Simplified Flow Diagram of Time-Dependent Radiation Hydrodynamics Code

This flow diagram assumes that there exists a fully converged temperature distribution for a time $(t-\Delta t)$.

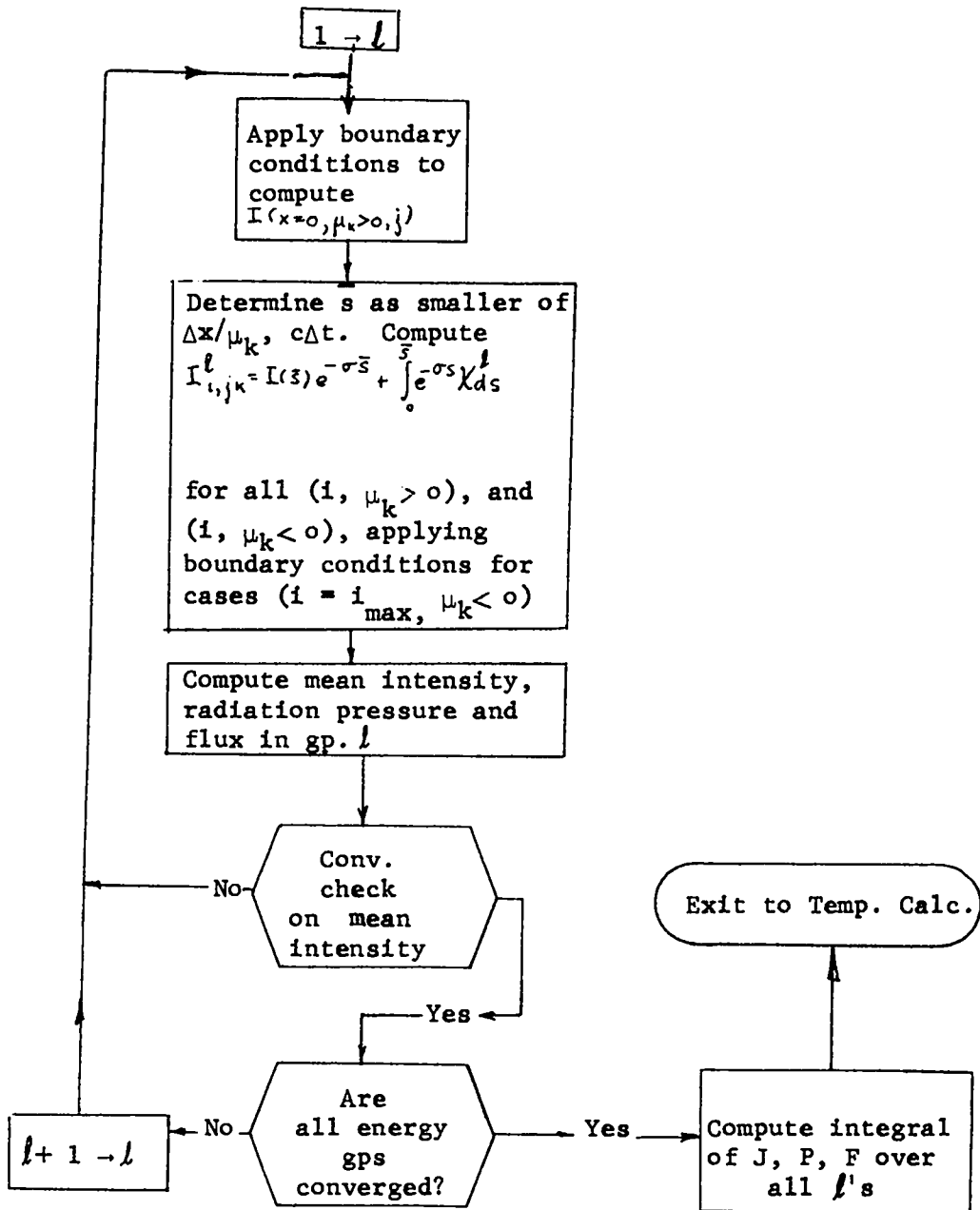


Fig. 6

Simplified Flow Diagram of Intensity Calculation
in Plane Geometry at Time $t = t_j$

4. NUMERICAL RESULTS

The problems discussed below are typical of many which may be of interest to astrophysicists. The primary reason for their inclusion is that each verifies the fact that a certain section of the code is without error.

Milne Problem

The Milne problem has been thoroughly discussed by Mark

(4). The equation to be solved is

$$\mu \frac{\partial I}{\partial x} + I = \frac{1}{2} \int_{-1}^1 I(x, \mu') d\mu'. \quad (4.1)$$

A solution is sought in the semi-infinite half-space $x \geq 0$ subject to the boundary condition,

$$I(0, \mu > 0) = 0. \quad (4.2)$$

A trial function,

$$I(x, \mu) = \frac{3}{2} (x - \mu), \quad (4.3)$$

which satisfies (4.1), but not (4.2), was inserted as a zeroth guess and the iteration was carried forward until the flux F satisfied the condition

$$F = 2\pi \int_{-1}^1 I d\mu = \text{const.} \quad (4.4)$$

That the condition (4.4) holds is readily verified by multiplying (4.1) by μ and then integrating over all μ . The constant

3/2 was chosen in (4.3) to normalize the flux to 2π .

Table 2 is the listing. It will be observed that the flux is not constant, varying about 15 parts in 600, with a particularly sharp drop at the boundary $x = 0$. The reason for this is that a quantity x_0 , known as the extrapolated length, has not been calculated with any great accuracy in the present case. If normalized properly, the radiation pressure at $x = 0$ is given by

$$p(0) = x_0 = .71044609..$$

To compare this number with our listing, we have

$$p(0) = \frac{2\pi}{c} x_0 = 1.46826 \times 10^{-10}$$

so that

$$x_0 \approx .70107$$

in error about one part in 70. Mark (4) has shown that the extrapolated length must be known with extreme accuracy if the flux and the mean intensity are to be accurately known. By juggling with our trial function, we are able to arrive (slowly) at values of the flux which are more constant than the one listed herein. However, the process is slow and an improvement in the method of energy check (used in the following problems) will yield more rapidly convergent (and constant) values of the flux.

Gray Body Atmosphere

The equation under discussion is

$$\mu \frac{\partial I}{\partial x} + I = B(T), \quad (4.5)$$

TABLE 2: LISTING FOR THE MILNE PROBLEM

INTENSITY ITER. NO.	1	DIFF= 3.09796-05		$\mu_3 = -\mu_2$	$\mu_4 = -\mu_1$	$\int_{-1}^1 I d\mu$	$\frac{2\pi}{C} \int_{-1}^1 \mu^2 I d\mu$	$2\pi \int_{-1}^1 \mu I d\mu$	DENSITY	TEMP
T= 3.6000+01	NU= 1.0000+00	PROB.NO.	3.							
I	X(I)	I(MU1)	I(MU2)	I(MU3)	I(MU4)	J(I)	P(I)	F(I)	RHO(I+1/2)	T(I+1/2)
0.	0.0000+00	0.0000+00	0.0000+00	1.2211+00	2.1561+00	1.6886+00	1.4630-10	-6.1528+00	1.0000+00	0.0000+00
1.	5.0000-01	6.3068-01	1.3224+00	2.0774+00	2.9594+00	3.4949+00	2.4999-10	-6.2711+00	1.0000+00	0.0000+00
2.	1.0000+00	1.3581+00	2.1908+00	2.8508+00	3.7220+00	5.0608+00	3.5483-10	-6.2952+00	1.0000+00	0.0000+00
3.	1.5000+00	2.1052+00	2.9666+00	3.6073+00	4.4763+00	6.5777+00	4.5990-10	-6.3002+00	1.0000+00	0.0000+00
4.	2.0000+00	2.8564+00	3.7237+00	4.3604+00	5.2290+00	8.0847+00	5.6507-10	-6.3013+00	1.0000+00	0.0000+00
5.	2.5000+00	3.6084+00	4.4769+00	5.1129+00	5.9813+00	9.5897+00	6.7015-10	-6.3017+00	1.0000+00	0.0000+00
6.	3.0000+00	4.3605+00	5.2293+00	5.8652+00	6.7336+00	1.1094+01	7.7529-10	-6.3018+00	1.0000+00	0.0000+00
7.	3.5000+00	5.1127+00	5.9816+00	6.6175+00	7.4858+00	1.2599+01	8.8043-10	-6.3020+00	1.0000+00	0.0000+00
8.	4.0000+00	5.8649+00	6.7339+00	7.3698+00	8.2381+00	1.4103+01	9.8557-10	-6.3021+00	1.0000+00	0.0000+00
9.	4.5000+00	6.6172+00	7.4863+00	8.1221+00	8.9904+00	1.5608+01	1.0907-09	-6.3023+00	1.0000+00	0.0000+00
10.	5.0000+00	7.3695+00	8.2386+00	8.8744+00	9.7428+00	1.7113+01	1.1959-09	-6.3024+00	1.0000+00	0.0000+00
11.	5.5000+00	8.1218+00	8.9909+00	9.6268+00	1.0495+01	1.8617+01	1.3010-09	-6.3025+00	1.0000+00	0.0000+00
12.	6.0000+00	8.8741+00	9.7433+00	1.0379+01	1.1247+01	2.0122+01	1.4062-09	-6.3026+00	1.0000+00	0.0000+00
13.	6.5000+00	9.6264+00	1.0496+01	1.1132+01	1.2000+01	2.1627+01	1.5113-09	-6.3026+00	1.0000+00	0.0000+00
14.	7.0000+00	1.0379+01	1.1248+01	1.1884+01	1.2752+01	2.3131+01	1.6165-09	-6.3026+00	1.0000+00	0.0000+00
15.	7.5000+00	1.1131+01	1.2000+01	1.2636+01	1.3504+01	2.4636+01	1.7216-09	-6.3026+00	1.0000+00	0.0000+00
16.	8.0000+00	1.1883+01	1.2753+01	1.3389+01	1.4257+01	2.6141+01	1.8268-09	-6.3025+00	1.0000+00	0.0000+00
17.	8.5000+00	1.2636+01	1.3505+01	1.4141+01	1.5009+01	2.7645+01	1.9319-09	-6.3023+00	1.0000+00	0.0000+00
18.	9.0000+00	1.3388+01	1.4258+01	1.4893+01	1.5761+01	2.9150+01	2.0370-09	-6.3020+00	1.0000+00	0.0000+00
19.	9.5000+00	1.4140+01	1.5010+01	1.5646+01	1.6513+01	3.0655+01	2.1422-09	-6.3016+00	1.0000+00	0.0000+00
20.	1.0000+01	1.4893+01	1.5762+01	1.6398+01	1.7265+01	3.2159+01	2.2473-09	-6.3012+00	1.0000+00	0.0000+00
21.	1.0500+01	1.5645+01	1.6514+01	1.7150+01	1.8017+01	3.3663+01	2.3524-09	-6.3006+00	1.0000+00	0.0000+00
22.	1.1000+01	1.6397+01	1.7266+01	1.7902+01	1.8769+01	3.5167+01	2.4575-09	-6.2999+00	1.0000+00	0.0000+00
23.	1.1500+01	1.7149+01	1.8019+01	1.8654+01	1.9521+01	3.6671+01	2.5626-09	-6.2991+00	1.0000+00	0.0000+00
24.	1.2000+01	1.7901+01	1.8771+01	1.9406+01	2.0273+01	3.8175+01	2.6677-09	-6.2981+00	1.0000+00	0.0000+00
25.	1.2500+01	1.8653+01	1.9522+01	2.0158+01	2.1024+01	3.9679+01	2.7728-09	-6.2969+00	1.0000+00	0.0000+00
26.	1.3000+01	1.9405+01	2.0274+01	2.0909+01	2.1776+01	4.1182+01	2.8778-09	-6.2956+00	1.0000+00	0.0000+00
27.	1.3500+01	2.0157+01	2.1026+01	2.1661+01	2.2527+01	4.2685+01	2.9829-09	-6.2942+00	1.0000+00	0.0000+00
28.	1.4000+01	2.0908+01	2.1777+01	2.2412+01	2.3278+01	4.4187+01	3.0878-09	-6.2925+00	1.0000+00	0.0000+00
29.	1.4500+01	2.1659+01	2.2528+01	2.3163+01	2.4028+01	4.5689+01	3.1928-09	-6.2907+00	1.0000+00	0.0000+00
30.	1.5000+01	2.2411+01	2.3279+01	2.3914+01	2.4779+01	4.7191+01	3.2978-09	-6.2886+00	1.0000+00	0.0000+00
31.	1.5500+01	2.3162+01	2.4030+01	2.4664+01	2.5529+01	4.8692+01	3.4026-09	-6.2864+00	1.0000+00	0.0000+00
32.	1.6000+01	2.3912+01	2.4780+01	2.5414+01	2.6279+01	5.0193+01	3.5075-09	-6.2839+00	1.0000+00	0.0000+00
33.	1.6500+01	2.4663+01	2.5531+01	2.6164+01	2.7028+01	5.1693+01	3.6123-09	-6.2813+00	1.0000+00	0.0000+00
34.	1.7000+01	2.5413+01	2.6280+01	2.6914+01	2.7777+01	5.3192+01	3.7171-09	-6.2784+00	1.0000+00	0.0000+00
35.	1.7500+01	2.6163+01	2.7030+01	2.7663+01	2.8526+01	5.4691+01	3.8218-09	-6.2752+00	1.0000+00	0.0000+00
36.	1.8000+01	2.6912+01	2.7779+01	2.8412+01	2.9274+01	5.6188+01	3.9265-09	-6.2718+00	1.0000+00	0.0000+00
37.	1.8500+01	2.7661+01	2.8528+01	2.9160+01	3.0022+01	5.7685+01	4.0311-09	-6.2682+00	1.0000+00	0.0000+00
38.	1.9000+01	2.8410+01	2.9276+01	2.9908+01	3.0769+01	5.9181+01	4.1356-09	-6.2644+00	1.0000+00	0.0000+00
39.	1.9500+01	2.9158+01	3.0024+01	3.0654+01	3.1516+01	6.0676+01	4.2401-09	-6.2605+00	1.0000+00	0.0000+00
40.	2.0000+01	2.9906+01	3.0770+01	3.1397+01	3.2263+01	6.2168+01	4.3445-09	-6.2570+00	0.0000+00	0.0000+00

$\mu_1 = .78867514$

$\mu_2 = .2132487$

where $B(T)$ is the temperature-dependent integrated Planck-function;

namely,

$$B(T) = \int_0^{\infty} \bar{B}^{\nu} d\nu = \frac{\sigma}{\pi} T^4(x). \quad (4.6)$$

Here, σ is the Stefan constant;

$$\sigma = 5.6724 \times 10^{-5} \text{ ergs/cm}^2\text{-sec-}(\text{°K})^4.$$

It will be noted that x is dimensionless; it is, properly, optical depth. The boundary conditions chosen were

$$\left. \begin{aligned} \bar{I}(10, -\mu) &= \frac{3}{4} F \cdot (10 + q(10) + |\mu|); \\ \bar{I}(0, \mu > 0) &= 0. \end{aligned} \right\} \quad (4.7)$$

The number $q(10) = .71044609$ is known as the extrapolated length.

One can determine the degree of consistency between the derived temperatures $T(x)$ and the constant flux F by application of the relation (5)

$$\sigma T^4 = \frac{3}{4} F \cdot (x + q(x)) \quad (4.8)$$

Calculations made using (4.8) to find $T(x)$ show that the listings of Table 3 are self-consistent to within a maximum difference of a few parts in a thousand.

Time Dependent Gray Body Atmosphere

The solution to

$$\frac{1}{c} \frac{\partial \bar{I}}{\partial t} + \mu \frac{\partial \bar{I}}{\partial x} + \bar{I} = B(T(x, t)) \quad (4.9)$$

with boundary conditions (4.7) and initial data

$$\bar{I}(x, 0) = T(x, 0) = 0 \quad (x > 0)$$

is required. As $t \rightarrow \infty$, the solution to (4.9) must approach the

TABLE 3: TIME INDEPENDENT GRAY BODY LISTING

T=1.4170+02 DT=2.0000-01 PROB. NO. 5

	OPTICAL DEPTH	VELOCITY	DENSITY	TEMP(°K)	RADIATION ENERGY DENSITY	RADIATION PRESSURE	FLUX	NET FLUX
I	X(I)	V(I)	RHO(I+1/2)	T(I+1/2)	E(I)	PR(I)	F(I)	NET F(I)
0.	0.000000+00	0.000000+00	1.000000+00	4.619996+03	2.828505+00	1.156891+00	-4.880040+10	-2.463864+04
1.	2.500000-C1	0.000000+00	1.000000+00	5.090557+03	4.392010+00	1.555774+00	-4.880042+10	-2.627702+04
2.	5.000000-C1	0.000000+00	1.000000+00	5.398528+03	5.745399+00	1.95892+00	-4.880045+10	-2.676670+04
3.	7.500000-C1	0.000000+00	1.000000+00	5.645085+03	7.044945+00	2.366066+00	-4.880048+10	-2.697407+04
4.	1.000000+00	0.000000+00	1.000000+00	5.859901+03	8.296987+00	2.773151+00	-4.880050+10	-2.695386+04
5.	1.250000+00	0.000000+00	1.000000+00	6.051724+03	9.531255+00	3.180242+00	-4.880053+10	-2.678056+04
6.	1.500000+00	0.000000+00	1.000000+00	6.226314+03	1.075796+01	3.587327+00	-4.880056+10	-2.648788+04
7.	1.750000+00	0.000000+00	1.000000+00	6.387122+03	1.198151+01	3.994411+00	-4.880058+10	-2.609922+04
8.	2.000000+00	0.000000+00	1.000000+00	6.536550+03	1.320373+01	4.401494+00	-4.880061+10	-2.563099+04
9.	2.250000+00	0.000000+00	1.000000+00	6.676354+03	1.442538+01	4.808576+00	-4.880064+10	-2.509584+04
10.	2.500000+00	0.000000+00	1.000000+00	6.807884+03	1.564680+01	5.215658+00	-4.880066+10	-2.450397+04
11.	2.750000+00	0.000000+00	1.000000+00	6.932204+03	1.686812+01	5.622740+00	-4.880069+10	-2.386387+04
12.	3.000000+00	0.000000+00	1.000000+00	7.050177+03	1.808940+01	6.029622+00	-4.880071+10	-2.318277+04
13.	3.250000+00	0.000000+00	1.000000+00	7.162511+03	1.931066+01	6.436503+00	-4.880073+10	-2.246690+04
14.	3.500000+00	0.000000+00	1.000000+00	7.269798+03	2.053191+01	6.843585+00	-4.880076+10	-2.172176+04
15.	3.750000+00	0.000000+00	1.000000+00	7.372537+03	2.175316+01	7.251067+00	-4.880078+10	-2.095218+04
16.	4.000000+00	0.000000+00	1.000000+00	7.471154+03	2.297441+01	7.658149+00	-4.880080+10	-2.016246+04
17.	4.250000+00	0.000000+00	1.000000+00	7.566016+03	2.419566+01	8.065231+00	-4.880082+10	-1.935649+04
18.	4.500000+00	0.000000+00	1.000000+00	7.657439+03	2.541691+01	8.472212+00	-4.880084+10	-1.853771+04
19.	4.750000+00	0.000000+00	1.000000+00	7.745701+03	2.663816+01	8.879394+00	-4.880086+10	-1.770930+04
20.	5.000000+00	0.000000+00	1.000000+00	7.831046+03	2.785940+01	9.286477+00	-4.880087+10	-1.687409+04
21.	5.250000+00	0.000000+00	1.000000+00	7.913690+03	2.908065+01	9.693559+00	-4.880089+10	-1.603469+04
22.	5.500000+00	0.000000+00	1.000000+00	7.993823+03	3.030190+01	1.010064+01	-4.880091+10	-1.519347+04
23.	5.750000+00	0.000000+00	1.000000+00	8.071617+03	3.152315+01	1.050772+01	-4.880092+10	-1.435259+04
24.	6.000000+00	0.000000+00	1.000000+00	8.147225+03	3.274440+01	1.091481+01	-4.880094+10	-1.351403+04
25.	6.250000+00	0.000000+00	1.000000+00	8.220785+03	3.396565+01	1.132189+01	-4.880095+10	-1.267961+04
26.	6.500000+00	0.000000+00	1.000000+00	8.292422+03	3.518690+01	1.172897+01	-4.880096+10	-1.185098+04
27.	6.750000+00	0.000000+00	1.000000+00	8.362250+03	3.640814+01	1.213605+01	-4.880097+10	-1.102966+04
28.	7.000000+00	0.000000+00	1.000000+00	8.430371+03	3.762939+01	1.254314+01	-4.880099+10	-1.021705+04
29.	7.250000+00	0.000000+00	1.000000+00	8.496881+03	3.885064+01	1.295022+01	-4.880100+10	-9.414427+03
30.	7.500000+00	0.000000+00	1.000000+00	8.561864+03	4.007189+01	1.335730+01	-4.880100+10	-8.622931+03
31.	7.750000+00	0.000000+00	1.000000+00	8.625400+03	4.129314+01	1.376438+01	-4.880101+10	-7.843609+03
32.	8.000000+00	0.000000+00	1.000000+00	8.687563+03	4.251438+01	1.417147+01	-4.880102+10	-7.077349+03
33.	8.250000+00	0.000000+00	1.000000+00	8.748419+03	4.373562+01	1.457555+01	-4.880103+10	-6.324857+03
34.	8.500000+00	0.000000+00	1.000000+00	8.808030+03	4.495685+01	1.498563+01	-4.880103+10	-5.586500+03
35.	8.750000+00	0.000000+00	1.000000+00	8.866456+03	4.617804+01	1.539272+01	-4.880104+10	-4.862168+03
36.	9.000000+00	0.000000+00	1.000000+00	8.923717+03	4.739913+01	1.579580+01	-4.880105+10	-4.149288+03
37.	9.250000+00	0.000000+00	1.000000+00	8.980048+03	4.862012+01	1.620089+01	-4.880105+10	-3.449000+03
38.	9.500000+00	0.000000+00	1.000000+00	9.034299+03	4.984009+01	1.661393+01	-4.880105+10	-2.713753+03
39.	9.750000+00	0.000000+00	1.000000+00	9.093737+03	5.106234+01	1.702126+01	-4.880106+10	-2.131463+03
40.	1.000000+C1	0.000000+00	0.000000+00	9.117100+03	5.231214+01	1.743534+01	-4.880106+10	0.000000+00

solution to the problem just completed. The listings of Table 4 can be compared with those of Table 3; they are virtually identical, Table 4 being taken from the listings at a time late enough so that equilibrium had been reached. Fig. 7 is a plot of the temperature distribution as a function of position for the times indicated and shows the way in which the temperature approaches its equilibrium value.

Time Dependent Gray Body with Hydrodynamics

The problem is similar to the last one solved, with the exception that hydrodynamic motions are now allowed. Again, we want the solution to

$$\frac{1}{c} \frac{\partial I}{\partial t} + \mu \frac{\partial I}{\partial x} + \rho(x,t) L = \rho(x,t) B, \quad (4.10)$$

where B is the integrated Planck function. The initial data are $\rho(x, t = 0) = 5 \times 10^{-8} \text{ cm}^{-1}$; $T(x,0)$ is given (it is unimportant and will not be listed here); each of twenty zones had an initial width of 10^7 cms . In addition, a gravitational acceleration of magnitude $g = 10^6 \text{ cm/sec}^2$ was inserted, resulting in the addition of such a term to the acceleration equation (3.21) (in the direction of negative x) and in the addition of a term $-|g| \Delta t (v_{i+1}^{j+1/2} + v_i^{j+1/2})/2$ to the right-hand-side of the energy balance equation (3.20).

The listings are lengthy and somewhat unsatisfactory in the sense that small oscillations in position, velocity, and other dependent variables persisted from a time $t \approx 100 \text{ sec}$ to $t = 336 \text{ sec}$.

TABLE 4: TIME DEPENDENT GRAY BODY LISTING: EQUILIBRIUM STATE

T= 1.4480+02 DT= 2.0000-01 PROB. NO. 6

I	OPTICAL DEPTH	VELOCITY	DENSITY	TEMP(*K)	RADIATION	RADIATION	FLUX	NET FLUX
	X(I)	V(I)	RHO(I+1/2)	T(I+1/2)	ENERGY DENSITY E(I)	PRESSURE PR(I)	F(I)	NET F(I)
0.	0.000000+00	0.000000+00	1.000000+00	4.619982+03	2.828472+00	1.156878+00	-4.879985+10	-5.753598+04
1.	2.500000-01	0.000000+00	1.000000+00	5.090542+03	4.391959+00	1.559757+00	-4.879991+10	-6.136185+04
2.	5.000000-01	0.000000+00	1.000000+00	5.398512+03	5.749333+00	1.958671+00	-4.879997+10	-6.250528+04
3.	7.500000-01	0.000000+00	1.000000+00	5.645069+03	7.044866+00	2.366040+00	-4.880003+10	-6.298946+04
4.	1.000000+00	0.000000+00	1.000000+00	5.859885+03	8.296898+00	2.773122+00	-4.880009+10	-6.294220+04
5.	1.250000+00	0.000000+00	1.000000+00	6.051708+03	9.531155+00	3.180210+00	-4.880016+10	-6.253745+04
6.	1.500000+00	0.000000+00	1.000000+00	6.226296+03	1.075786+01	3.587292+00	-4.880022+10	-6.185395+04
7.	1.750000+00	0.000000+00	1.000000+00	6.387106+03	1.198139+01	3.994373+00	-4.880028+10	-6.094630+04
8.	2.000000+00	0.000000+00	1.000000+00	6.536534+03	1.320360+01	4.401453+00	-4.880034+10	-5.985284+04
9.	2.250000+00	0.000000+00	1.000000+00	6.676339+03	1.442525+01	4.808534+00	-4.880040+10	-5.860313+04
10.	2.500000+00	0.000000+00	1.000000+00	6.807869+03	1.564667+01	5.215614+00	-4.880046+10	-5.722097+04
11.	2.750000+00	0.000000+00	1.000000+00	6.932190+03	1.686798+01	5.622694+00	-4.880052+10	-5.572618+04
12.	3.000000+00	0.000000+00	1.000000+00	7.050163+03	1.808926+01	6.029775+00	-4.880057+10	-5.413564+04
13.	3.250000+00	0.000000+00	1.000000+00	7.162498+03	1.931052+01	6.436855+00	-4.880063+10	-5.246394+04
14.	3.500000+00	0.000000+00	1.000000+00	7.269785+03	2.053177+01	6.843936+00	-4.880068+10	-5.072387+04
15.	3.750000+00	0.000000+00	1.000000+00	7.372525+03	2.175301+01	7.251018+00	-4.880073+10	-4.892674+04
16.	4.000000+00	0.000000+00	1.000000+00	7.471142+03	2.297426+01	7.658099+00	-4.880078+10	-4.708260+04
17.	4.250000+00	0.000000+00	1.000000+00	7.566004+03	2.419551+01	8.065181+00	-4.880083+10	-4.520048+04
18.	4.500000+00	0.000000+00	1.000000+00	7.657428+03	2.541676+01	8.472263+00	-4.880087+10	-4.328849+04
19.	4.750000+00	0.000000+00	1.000000+00	7.745690+03	2.663801+01	8.879346+00	-4.880091+10	-4.135399+04
20.	5.000000+00	0.000000+00	1.000000+00	7.831036+03	2.785926+01	9.286428+00	-4.880096+10	-3.940363+04
21.	5.250000+00	0.000000+00	1.000000+00	7.913680+03	2.908051+01	9.693511+00	-4.880100+10	-3.744348+04
22.	5.500000+00	0.000000+00	1.000000+00	7.993814+03	3.030176+01	1.010059+01	-4.880103+10	-3.547907+04
23.	5.750000+00	0.000000+00	1.000000+00	8.071608+03	3.152301+01	1.050768+01	-4.880107+10	-3.351547+04
24.	6.000000+00	0.000000+00	1.000000+00	8.147217+03	3.274426+01	1.091476+01	-4.880110+10	-3.155729+04
25.	6.250000+00	0.000000+00	1.000000+00	8.220777+03	3.396552+01	1.132185+01	-4.880113+10	-2.960877+04
26.	6.500000+00	0.000000+00	1.000000+00	8.292415+03	3.518677+01	1.172893+01	-4.880116+10	-2.767377+04
27.	6.750000+00	0.000000+00	1.000000+00	8.362243+03	3.640802+01	1.213601+01	-4.880119+10	-2.575586+04
28.	7.000000+00	0.000000+00	1.000000+00	8.430365+03	3.762928+01	1.254310+01	-4.880122+10	-2.385830+04
29.	7.250000+00	0.000000+00	1.000000+00	8.496875+03	3.885053+01	1.295018+01	-4.880124+10	-2.198404+04
30.	7.500000+00	0.000000+00	1.000000+00	8.561859+03	4.007179+01	1.335727+01	-4.880126+10	-2.013578+04
31.	7.750000+00	0.000000+00	1.000000+00	8.625396+03	4.129304+01	1.376435+01	-4.880128+10	-1.831593+04
32.	8.000000+00	0.000000+00	1.000000+00	8.687559+03	4.251430+01	1.417144+01	-4.880130+10	-1.652660+04
33.	8.250000+00	0.000000+00	1.000000+00	8.748416+03	4.373554+01	1.457852+01	-4.880132+10	-1.476942+04
34.	8.500000+00	0.000000+00	1.000000+00	8.808026+03	4.495677+01	1.498561+01	-4.880133+10	-1.304524+04
35.	8.750000+00	0.000000+00	1.000000+00	8.866453+03	4.617797+01	1.539270+01	-4.880135+10	-1.135385+04
36.	9.000000+00	0.000000+00	1.000000+00	8.923715+03	4.739908+01	1.579978+01	-4.880136+10	-9.689149+03
37.	9.250000+00	0.000000+00	1.000000+00	8.980046+03	4.86207+01	1.620687+01	-4.880137+10	-8.053883+03
38.	9.500000+00	0.000000+00	1.000000+00	9.034297+03	4.984005+01	1.661392+01	-4.880137+10	-6.336977+03
39.	9.750000+00	0.000000+00	1.000000+00	9.093735+03	5.106231+01	1.702125+01	-4.880138+10	-4.977252+03
40.	1.000000+01	0.000000+00	0.000000+00	9.117100+03	5.231213+01	1.743533+01	-4.880139+10	0.000000+00

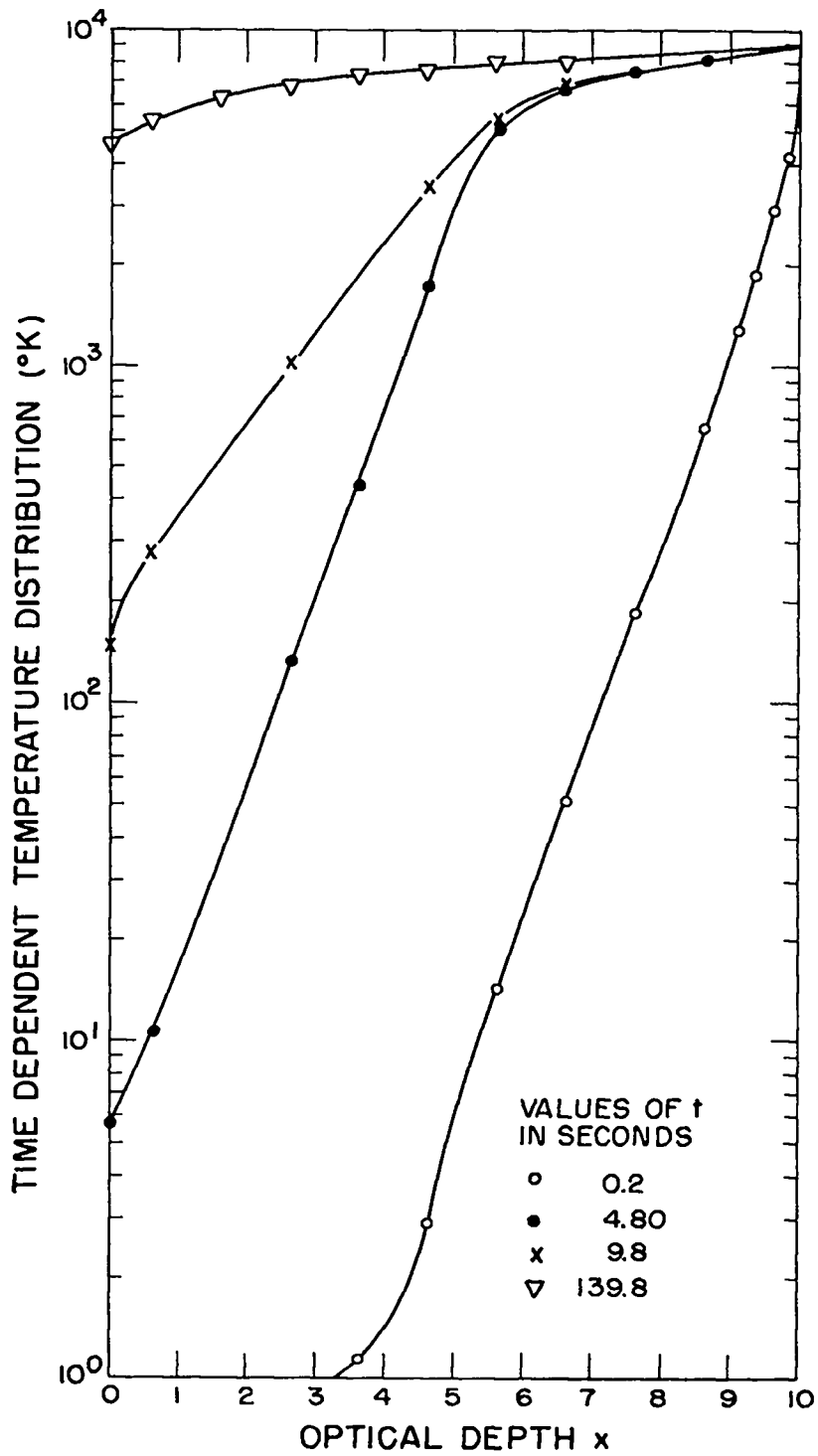


Fig. 7

The Time Behavior of the Temperature "Wave" in a Gray Body

The oscillations in the velocity were of the order of 10 meters/sec, while the peak velocity, as seen from Fig. 8, was of the order of 30 - 40 kms/sec for most of the outer zones. The temperature distribution at 336 seconds was within a percent or two (for all x) of the equilibrium distribution of the time independent gray body atmosphere. Fig. 9 shows the time development of the temperature toward its equilibrium value. The density, originally a constant for the initial distance of 2×10^8 cms, showed the time behavior given in Fig. 10. The oscillations in values of the density within any zone were of the order of a few percent about the values shown at $t = 170$ sec. The oscillations in the flux were rather more serious than those in temperature, density, and velocity. This is to be expected since the flux is proportional to the fourth power of temperature. Nevertheless, at $t = 357$ sec, the extreme values of the flux were 4.69894×10^{10} ergs/cm² - sec and 4.855346×10^{10} ergs/cm² - sec, the values tending to concentrate about 4.82×10^{10} ergs/cm² - sec. The last value quoted is about one percent lower than the 4.88×10^{10} ergs/cm² - sec found in the two problems immediately preceding the present one, while the maximum spread from minimum to maximum values of flux is of the order of 3.2%.

5. CONCLUDING REMARKS

Future work with the code described herein will be pointed toward making many of the subroutines more general than they are at

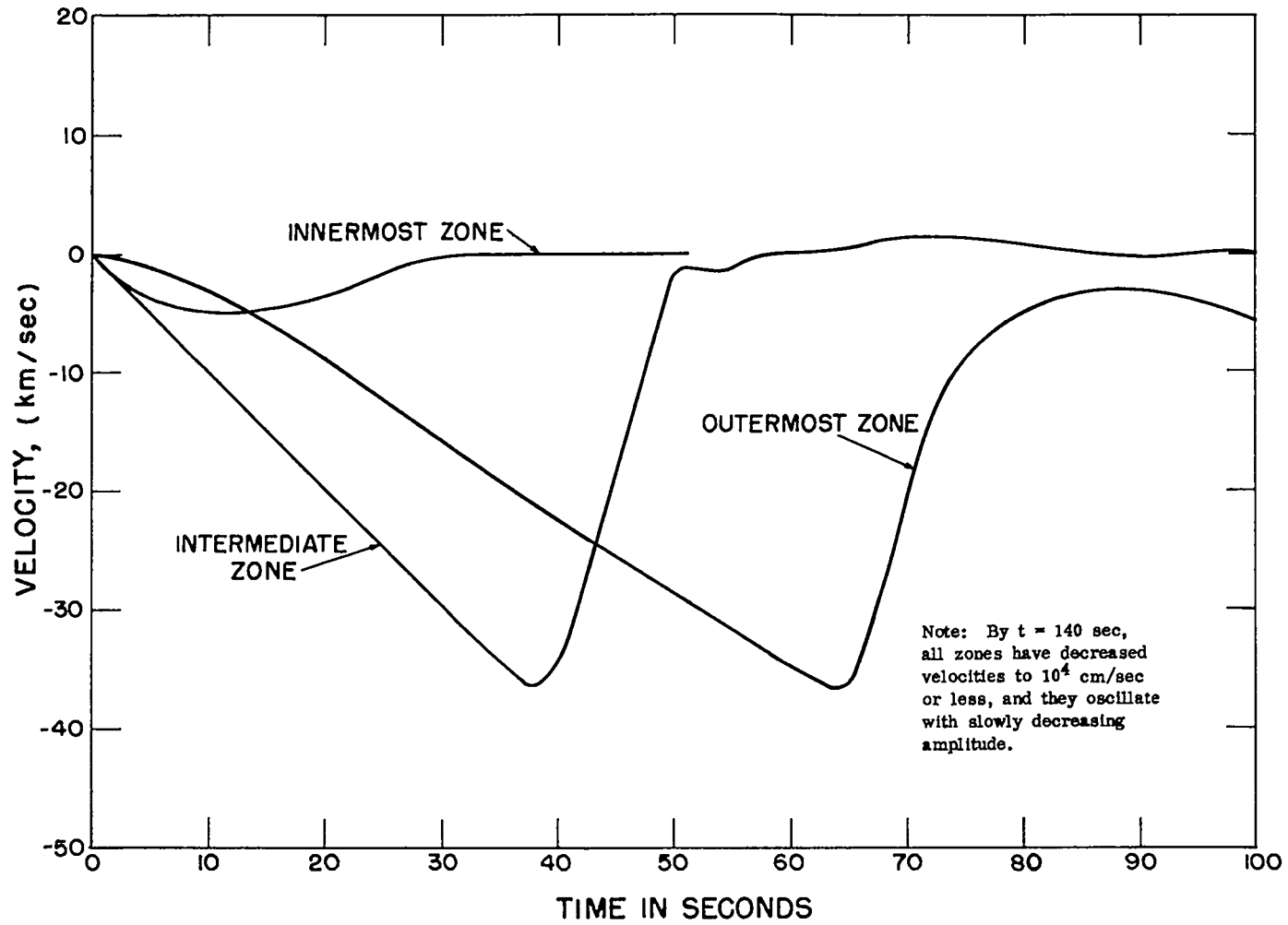


Fig. 8

The Time Behavior of the Velocity of the Zones Indicated

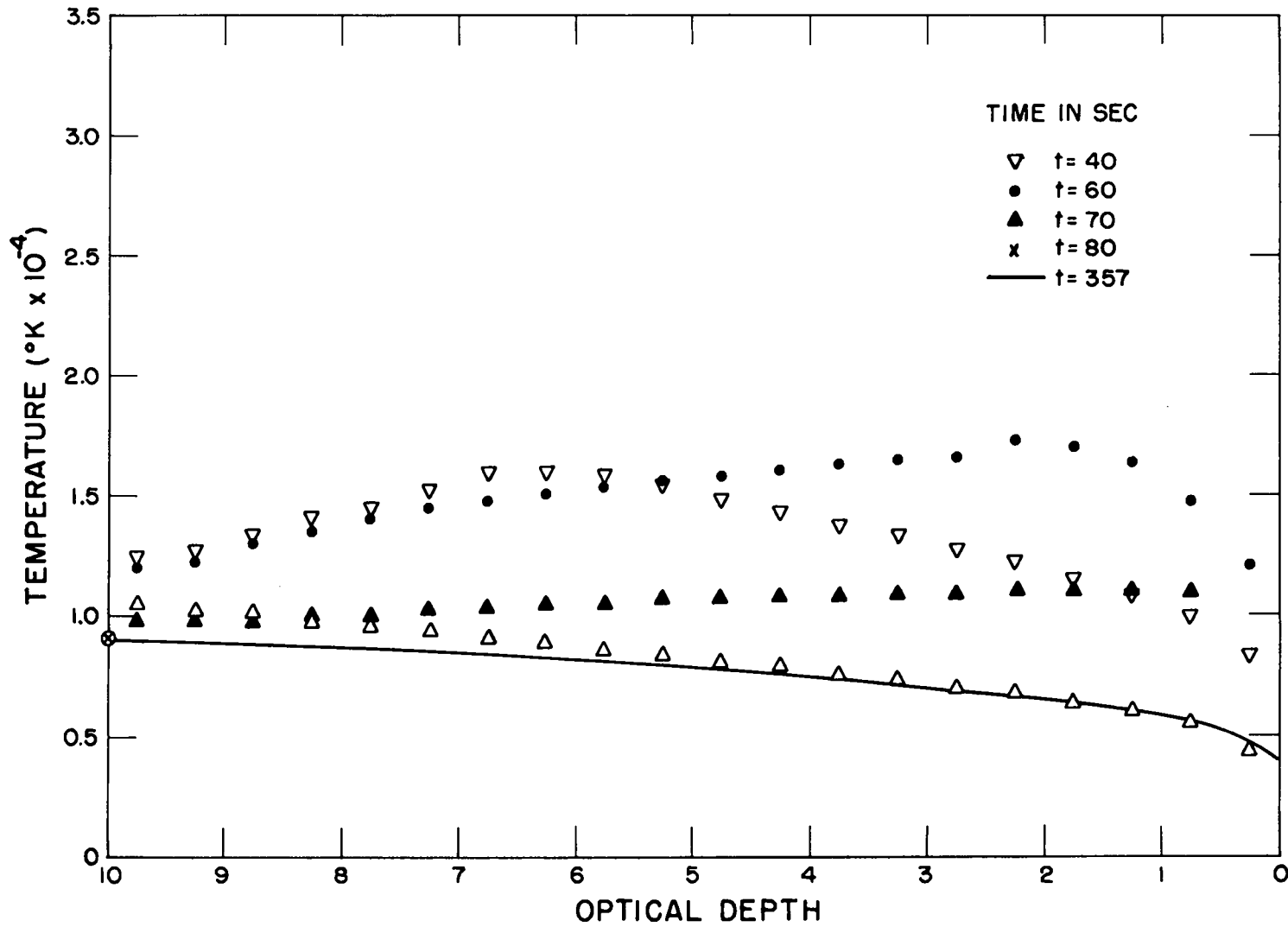


Fig. 9

Temperature Profiles at Indicated Times, Showing Approach to Equilibrium

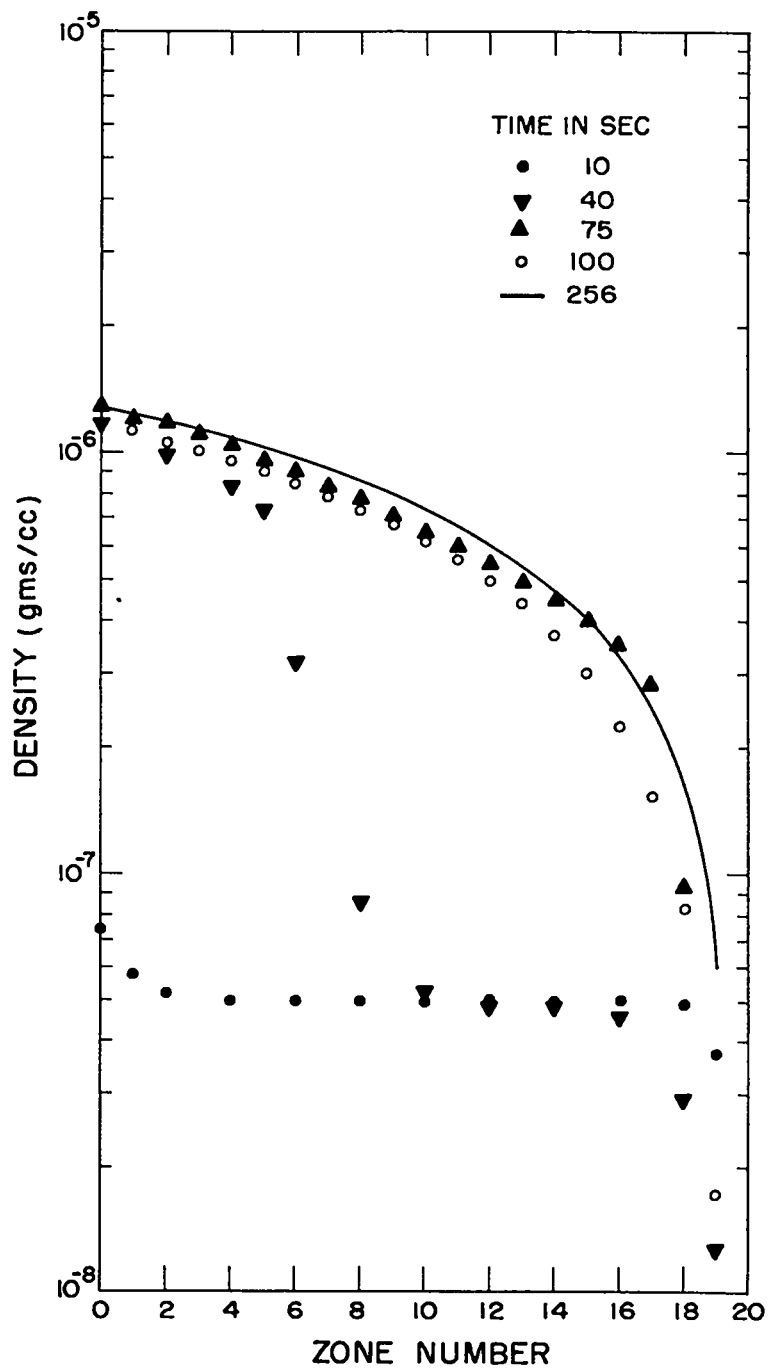


Fig. 10

Density Profiles at Indicated Times,
 Showing Approach to Equilibrium

present. For example, we shall use more general equations of state, together with variable specific heats. Although an earlier 7090 version of this code was able to read a variety of input data from tape, the present one must have such a feature built into it.

We want to conduct numerical experiments designed to test the relative amount of time required for convergence of a problem with given hydrodynamic input when linear versus quadratic viscous pressures are used. Another numerical test of some significance which will be investigated is the one which involves assuming the temperature a constant only for purposes of computing absorption.

That is, if one must evaluate the integral,

$$\phi = \int_0^{\Delta x/\mu} \sigma_a (T(x', t - \frac{x'}{c})) dx',$$

which occurs in the form $e^{-\phi}$, we can, if $\Delta x/\mu$ is not too large,

use T at the point $\frac{\Delta x}{2\mu}$ as an approximation for T throughout the zone.

This would make computation somewhat faster. Other ways of speeding the operation of the code are envisaged, but will not be discussed here.

REFERENCES

1. L. H. Thomas, Quart. J. Math, Oxford 1, 239 (1930),
2. A. N. Fraser, AWRE, TPN 77/58, 78/58, 95/59.
3. P. Ledoux and Th. Walraven, Handbuch der Physik, Fol. 51, 353 (esp. pgs. 442 et seq.), Springer - Verlag, 1958.
4. C. Mark, Phys. Rev. 72, 558, (1947).
5. V. Kourganoff, Basic Methods in Transfer Problems, Oxford, 1952, pg. 135.